Science World Journal Vol. 19(No 4) 2024 https://dx.doi.org/10.4314/swj.v19i4.14
www.scienceworldjournal.org
ISSN: 1597-6343 (Online), ISSN: 2756-391X (Print)
Published by Faculty of Science, Kaduna State University

Full Length Research Article

PREPARATION AND CHARACTERIZATION OF MoO_3 NANOPARTICLES FOR THE PHOTOCATALYTIC DEGRADATION OF DYEING WASTEWATER

Idris A. Yakubu, Elele U. Ugoeze and *John T. Mathew

Department of Chemistry, Ibrahim Badamasi Babangida University, Lapai, Niger State, Nigeria

*Corresponding Author Email Address: johntsadom@gmail.com

ABSTRACT
This study focuses on the preparation and characterization of MoO_3 nanoparticles for the photocatalytic degradation of dyeing wastewater. The XRD pattern of MoO_3 shows distinct peaks at 2θ values of 12.8°, 23.4°, 25.7°, 27.3°, and 39.0°, corresponding to specific crystal planes and confirming its α-MoO_3 phase, validated against JCPDS card number 05-0508. The morphology reveals stacked or crumpled particles with a high surface area conducive to catalytic activities. EDX analysis identifies molybdenum (Mo) and oxygen (O) with characteristic peaks at 2.29 keV (Mo Lα), 17.48 keV (Mo Kα), 19.63 keV (Mo Kβ), and 0.52 keV (O Kα), confirming the material's composition. MoO_3's layered structure, influenced by van der Waals forces, offers unique interlayer spacing advantageous for photocatalytic processes. Photodegradation experiments showed progressive efficiency: at 10 minutes, MoO_3 achieved 8.58%; by 40 minutes, it increased to 30.42%, and at 50 minutes, reached 42.3%. Efficiency peaked at 60 minutes with 50.52%, progressing to 60.8% at 70 minutes and 71.03% at 90 minutes, finally achieving 75.25% at 100 minutes. These results demonstrate MoO_3 nanoparticles' effectiveness in degrading dye pollutants, highlighting their potential for sustainable wastewater treatment applications.

Keywords: characteristic, degradation, MoO_3, nanoparticles, photocatalytic, wastewater

INTRODUCTION

The increasing production of textile goods has led to a substantial rise in dyeing wastewater, which is one of the most challenging types of industrial effluents to treat. Dyeing wastewater typically contains high concentrations of synthetic dyes, surfactants, organic chemicals, and toxic heavy metals. These contaminants are not only resistant to conventional wastewater treatment methods but also pose significant environmental and health risks due to their persistence, toxicity, and potential for bioaccumulation. The release of untreated dyeing wastewater into water bodies leads to severe issues, such as the depletion of dissolved oxygen, reduced light penetration, and the disruption of aquatic ecosystems. Therefore, there is an urgent need for advanced treatment technologies that can effectively remove these complex pollutants. Among the various approaches, photocatalysis has emerged as a promising technique due to its ability to utilize sunlight or artificial light to degrade organic pollutants into non-toxic byproducts. In this context, molybdenum trioxide (MoO_3) nanoparticles have attracted significant interest as efficient photocatalysts for the degradation of dyeing wastewater (Alsukaibi , 2022; Periyasamy, 2024).

Molybdenum trioxide (MoO_3) is a versatile transition metal oxide known for its high thermal stability, unique electronic properties, and strong oxidative capabilities. As a semiconductor material, MoO_3 exhibits a wide band gap, typically around 2.7 to 3.0 eV, which makes it suitable for photocatalytic applications under ultraviolet (UV) or visible light irradiation. The nanoscale form of MoO_3 offers enhanced surface area, increased reactivity, and a greater number of active sites, making it an excellent candidate for environmental remediation, particularly for the photocatalytic degradation of organic dyes. Recent advancements in nanotechnology have enabled the synthesis of MoO_3 nanoparticles with controlled size, shape, and morphology, leading to improved photocatalytic performance. Moreover, MoO_3 nanoparticles can generate reactive oxygen species (ROS) such as hydroxyl radicals (•OH) and superoxide anions (O_2^{-}•) upon light excitation, which play a crucial role in the oxidative degradation of pollutants (da Silva-Júnior *et al.* 2023, Qing *et al.* 2023).

The preparation of MoO_3 nanoparticles generally involves various synthesis methods, including hydrothermal, sol-gel, and chemical vapor deposition techniques. Among these, the hydrothermal method is widely favored due to its simplicity, cost-effectiveness, and ability to produce nanoparticles with uniform size and morphology. In this process, molybdenum precursors, such as ammonium molybdate, are dissolved in an aqueous solution and subjected to high temperature and pressure conditions, leading to the formation of MoO_3 nanocrystals. Key synthesis parameters like temperature, pH, precursor concentration, and reaction time play a critical role in determining the structural properties of the resulting nanoparticles. Advanced synthesis approaches, such as microwave-assisted hydrothermal and template-assisted methods, have also been explored to fine-tune the size and morphology of MoO_3 nanoparticles, further enhancing their photocatalytic efficiency (Gavrilova *et al.* 2020).

Characterization of MoO_3 nanoparticles is essential for understanding their structural, optical, and catalytic properties, which directly influence their photocatalytic activity. Techniques such as X-ray diffraction (XRD), scanning electron microscopy (SEM), and transmission electron microscopy (TEM) are commonly employed to determine the crystal structure, particle size, and morphology of the synthesized nanoparticles. Fourier-transform infrared spectroscopy (FTIR) and Raman spectroscopy provide insights into the functional groups and molecular vibrations, while UV-Vis diffuse reflectance spectroscopy (UV-Vis DRS) is used to assess the optical properties and band gap energy of the nanoparticles. Additionally, Brunauer-Emmett-Teller (BET) analysis helps evaluate the specific surface area, which is a critical factor affecting the photocatalytic performance. The comprehensive characterization of MoO_3 nanoparticles aids in correlating their structural features with their catalytic efficiency, facilitating the design of more effective materials for wastewater

treatment (Dargahi *et al.* 2020; Inobeme *et al.* 2023).

The photocatalytic degradation process using MoO_3 nanoparticles involves the absorption of photons, leading to the excitation of electrons from the valence band to the conduction band, creating electron-hole pairs. These charge carriers interact with water and oxygen molecules, generating ROS that degrade the dye molecules into smaller, non-toxic compounds such as CO_2 and H_2O. MoO_3 nanoparticles have demonstrated high photocatalytic activity against a wide range of dyes, including methylene blue, rhodamine B, and methyl orange, making them suitable for treating complex dye mixtures in wastewater. Furthermore, the photocatalytic process can be optimized by modifying the surface of MoO_3 nanoparticles with metal or non-metal dopants, enhancing their light absorption, charge separation, and stability under irradiation. The recyclability and reusability of MoO_3 nanoparticles also contribute to their potential as a sustainable solution for wastewater treatment (Hendrix *et al.* 2023).

In addition, the preparation and characterization of MoO_3 nanoparticles hold significant promise for the efficient photocatalytic degradation of dyeing wastewater. The unique properties of MoO_3, including its strong oxidative capability, high stability, and tunable optical features, make it an excellent photocatalyst for environmental applications. The optimization of synthesis methods and the detailed characterization of the nanoparticles are crucial for achieving high photocatalytic performance. As research progresses, the development of advanced MoO_3-based nanocomposites and hybrid materials may further enhance the efficiency and scalability of this approach, paving the way for practical applications in industrial wastewater treatment and contributing to cleaner and safer water resources (Dostanić *et al.* 2024).

MATERIAL AND METHODS

The dye wastewater used in this study was collected from one of the Textile Industries at the Industrial Estate in Kaduna State. The wastewater was collected from the wastewater tank before being discharged. The sample collected was brought to the laboratory and in diluted trioxonitrate(V) acid for analysis (Mathew et al. 2024a).

Synthesis of MoO_3 nanoparticles via sol-gel method

Precisely 50 grams of molybdenum nitrate tetraoxomanganese(VII) into a 250 cm^3 beaker, where approximately 100.0 cm^3 of de-ionized water to the beaker. The solution was placed in a magnetic stirrer to agitate the solution for 30 minutes at a rate of 150 revolutions per minute (rpm). 0.5 M sodium hydroxide (NaOH) was introduced into the solution in a dropwise manner, achieve the desired pH levels of 12. After stirring for 5 minutes, a precipitate was form. This precipitate was meticulously separated through filtration, by using Whatman No. 1 filter paper. The collected precipitate was thoroughly washed with deionized water and ethanol to eliminate any residual, unreacted precursors. Subsequently, the final product was subjected to drying in an oven set at 105 °C for 24 hours. After the drying process, the product was subjected to calcination in a furnace, maintained at a temperature of 450 °C. This calcination process is essential to produce nanoparticles (Mathew *et al.* 2024b).

Characterization of MoO_3 Nanoparticles

The zeolite-A, nanoparticles was characterized using different analytical instruments such as XRD, HRSEM, and HRTEM coupled with EDS and BET (Mathew *et al.* 2023a)

Effect of time

The effect of time on dye removal efficiency was investigated. A fixed concentration of dye solution was prepared and mixed with a predetermined amount of MoO_3 nanoparticles. The mixture was irradiated under simulated sunlight in a photoreactor. Aliquots of the solution were collected at regular intervals (e.g., 10, 20, 30, and 60 minutes) and immediately centrifuged to separate the catalyst. The supernatant was analyzed using a UV-Vis spectrophotometer to measure the absorbance at the dye's characteristic wavelength, determining the degradation percentage over time (Mathew *et al.* 2023b).

Effect of catalyst loading

To evaluate the effect of catalyst loading on photocatalytic degradation, MoO_3 nanoparticles were dispersed in 100 mL of dyeing wastewater at varying concentrations (0.1 g/L, 0.2 g/L, 0.3 g/L, and 0.5 g/L). The suspension was stirred and irradiated under simulated sunlight using a 300 W xenon lamp. Samples were collected at regular intervals and analyzed using a UV-Vis spectrophotometer to monitor dye concentration. The degradation efficiency was calculated, and the optimal catalyst loading was determined by the maximum removal efficiency achieved with minimal catalyst waste (Sinar-Mashuri ***et al.*** 2020).

Effect of pH

To investigate the effect of pH on photocatalytic degradation, the pH of dyeing wastewater solutions was adjusted to 3, 5, 7, 9, and 11 using dilute HCl or NaOH solutions. A fixed concentration of the dye solution was prepared, and 0.1 g of MoO_3 nanoparticles was added as the photocatalyst. The solutions were stirred in the dark for 30 minutes to establish adsorption equilibrium before exposure to simulated sunlight. Aliquots were collected at regular intervals, filtered, and analyzed using a UV-Vis spectrophotometer to monitor the degradation efficiency at different pH values (Mousavi *et al.* 2023).

RESULTS AND DISCUSSION

From fig. 1, MoO_3 exhibits an orthorhombic crystal structure, which is associated with the α-MoO_3 phase, the most stable and commonly observed form of MoO_3. The XRD pattern of MoO_3 is characterized by distinct peaks at 2θ values of 12.8°, 23.4°, 25.7°, 27.3°, and 39.0°, corresponding to the (020), (110), (021), (040), and (060) planes, consistent with JCPDS card number 05-0508, thus validating the phase identification of α-MoO_3 (Harini *et al.* 2022). Similarly, Norouzi *et al.* (2022) confirmed the presence of peaks corresponding to the orthorhombic α-MoO_3 structure in their XRD analysis. The low broadening of peaks can be attributed to lattice strain or the nanocrystalline nature of the material.

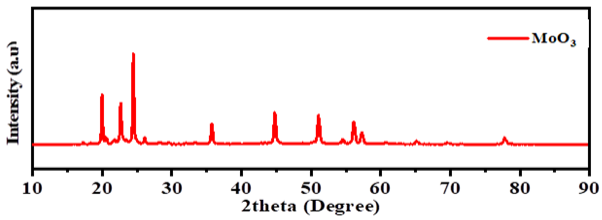

Figure 1: XRD Result of MoO_3 Nanoparticles

Science World Journal Vol. 19(No 4) 2024 https://dx.doi.org/10.4314/swj.v19i4.14
www.scienceworldjournal.org
ISSN: 1597-6343 (Online), ISSN: 2756-391X (Print)
Published by Faculty of Science, Kaduna State University

The HRSEM image of MoO_3 nanoparticles (Fig. 2) exhibits a layered orthorhombic crystal structure. These particles are stacked or crumpled, leading to a high surface area that is advantageous for catalytic activities (Jamil *et al.,* 2022). The HRSEM image also shows some degree of porosity, which further enhances the material's surface area.

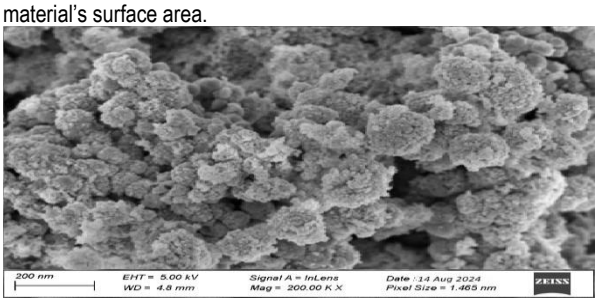

Figure 2: HRSEM image of MoO_3 nanoparticles

The EDX spectrum of MoO_3 (Fig. 3) features characteristic peaks for molybdenum (Mo) and oxygen (O). Molybdenum shows prominent peaks at approximately 2.29 keV (Mo Lα), 17.48 keV (Mo Kα), and 19.63 keV (Mo Kβ), while a peak represents oxygen at around 0.52 keV (O Kα), similar to ZnO. The peaks corresponding to molybdenum confirm the presence of MoO_3, with molybdenum in its +6 oxidation state. This is supported by the findings of Xiao et al. (2024), who noted the versatility of molybdenum in different oxidation states, including +6, and its implications in various chemical reactions (Xiao, *et al.* 2024).

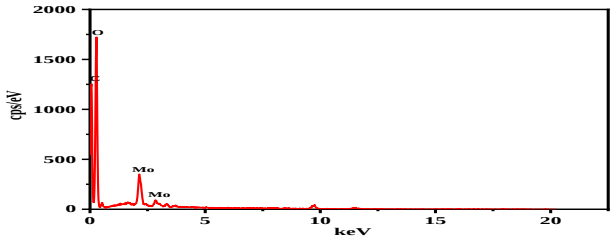

Figure 3: EDX image of MoO_3 nanoparticles

The HRTEM image of MoO_3 (Fig. 4) reveals layered structures due to the orthorhombic crystal structure. The lattice fringes corresponding to the (021) and (110) planes are typically visible, reflecting the anisotropic nature of MoO_3. The interlayer spacing in MoO_3 is generally larger compared to ZnO, which is a characteristic feature of its layered structure by the presence of van der Waals forces that bind the MoO_3 octahedra together, forming bi-layer structures (Papadimitropoulos *et al.* 2022). The high crystallinity of MoO_3, as evidenced by the clear lattice fringes, is also essential for its photocatalytic activity, particularly in facilitating intercalation and deintercalation processes that are critical for photocatalysis. The SAED pattern of MoO_3 usually shows diffraction rings or spots corresponding to the orthorhombic structure. The presence of diffraction rings, rather than spots, can indicate the polycrystalline nature of MoO_3, where multiple crystallites with random orientations contribute to the diffraction pattern. This polycrystallinity arises from the aggregation of multiple crystallites with random orientations, which contributes to the observed diffraction patterns (Larciprete, 2024). The diffraction rings are often indexed to planes such as (021), (110), and (111), which are characteristic of orthorhombic MoO_3. The polycrystalline nature of MoO_3, as observed in SAED, suggests that it may possess a higher density of grain boundaries, which can act as active sites for photocatalysis.

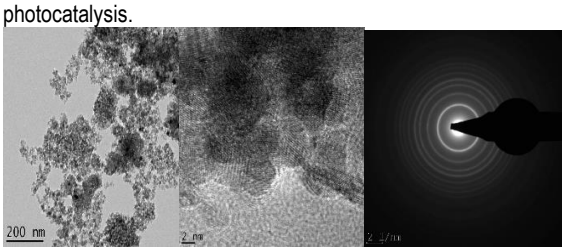

Figure 4: HRTEM and SAED Images of MoO_3

Table 1 presents some parameters analysed in dyeing wastewater. The high COD value of 1525.8 mg/L obtained indicates that the dyeing wastewater contains a significant amount of oxidizable pollutants, such as dyes, surfactants, and other organic compounds used in the dyeing process. This high COD level suggests a substantial organic load, which can lead to oxygen depletion in receiving water bodies, adversely affecting aquatic life (Mohamed *et al.,* 2022; Saha *et al.,* 2022). The BOD value of 252.43 mg/L is relatively high, indicating the presence of biodegradable organic compounds in the wastewater. While this value is lower than the COD, the significant difference between COD and BOD suggests that a large portion of the organic matter is not easily biodegradable. High BOD levels can lead to oxygen depletion in water bodies, resulting in the death of aquatic organisms and the disruption of the ecosystem (Rudaru *et al.,* 2022). The pH of the dyeing wastewater is 6.61, which is slightly acidic. The pH level is crucial because it affects the solubility and toxicity of chemicals in the water. The slightly acidic nature of the wastewater could be due to the use of acidic dyes or other acidic chemicals in the dyeing process, which can lead to significant environmental concerns if not properly managed (Delletesse, 2023).

Table 1: Some Physiochemical Parameters of Dyeing Wastewater

Parameter	Value
COD (mg/L)	1525.8
BOD (mg/L)	252.43
pH	6.11
Cl^- (mg/L)	607.75
Alkalinity (mg/L)	325.12
TDS (mg/L)	1052.05
Turbidity (NTU)	57.2
Conductivity (µS/cm)	2025.5

The chloride concentration of 607.75 mg/L is relatively high, which can have detrimental effects on aquatic life and soil if the wastewater is discharged untreated. High chloride levels can lead to an increase in the salinity of water bodies, which affects the osmoregulation of aquatic organisms. Solomon (2023) has shown that even concentrations below 230 mg/L can negatively impact aquatic organisms, particularly in waters with low background calcium levels. The alkalinity of 325.12 mg/L indicates that the wastewater has a moderate capacity to buffer acidic inputs, which is important for maintaining a stable pH during treatment

Science World Journal Vol. 19(No 4) 2024 https://dx.doi.org/10.4314/swj.v19i4.14
www.scienceworldjournal.org
ISSN: 1597-6343 (Online), ISSN: 2756-391X (Print)
Published by Faculty of Science, Kaduna State University

processes. High alkalinity can be beneficial in neutralizing acids generated during biological treatment processes, but it can also indicate the presence of excessive chemicals used in the dyeing process, such as sodium carbonate (Kim *et al.,* 2020). Total Dissolved Solids (TDS) represent the combined content of all inorganic and organic substances dissolved in the water. The TDS value of 1052.05 mg/L suggests that the wastewater contains a significant amount of dissolved substances, including salts, minerals, and organic compounds. High TDS levels can affect the taste and quality of water and can lead to scaling in pipes and equipment (Wang, 2021). The turbidity value of 57.2 NTU (Nephelometric Turbidity Units) indicates that the wastewater contains a high level of suspended particles, such as dyes, fibers, and other colloidal matter. High turbidity can reduce light penetration in water bodies, affecting photosynthesis in aquatic plants and disrupting the aquatic food chain (Mukarugwiro *et al.,* 2023). The high conductivity value of 2025.5 µS/cm indicates a significant presence of dissolved ions, such as salts, acids, and bases, which are commonly found in dyeing wastewater. High conductivity can be harmful to aquatic life, as it can affect the osmotic pressure and ion exchange processes of organisms. The presence of these ions is not only a consequence of the dyeing processes but also reflects the complex interactions between dyes and other chemical substances used (Wang *et al.,* 2023).

Photodegradation of dyeing wastewater was measured at 10 min intervals, with the performance metrics expressed as percentages using MoO_3 (see Fig. 5). In the initial stage of photodegradation (0-30 min), the photocatalysts exhibited varying degrees of activity. At 10 min, MoO_3 achieved a photodegradation efficiency of 8.58%. Kedves et al. (2023) reported that the presence of MoO_3 in a heterojunction with ZnO not only enhances the photocatalytic efficiency but also extends the absorption spectrum into the visible range, thereby improving the overall performance of the composite material. As the irradiation time increased to 20 min, the photodegradation efficiencies of MoO_3 was 15.72%. Here, the trend observed at 10 min persisted with MoO_3. At 30 min, the photodegradation efficiency was 25.5% for MoO_3.

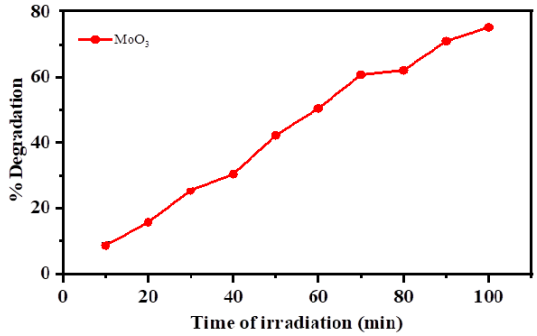

Figure 5: Effect of time using MoO_3 under UV-visible light

During the mid-stage of photodegradation (40-70 min), the differences in photocatalytic efficiency became more pronounced. At 40 min, the photodegradation efficiencies increased to 30.42 % for MoO_3. This anomaly could be due to the saturation of active sites on the composite material, which may have temporarily reduced its effectiveness. At 50 min, the photodegradation efficiencies rose significantly, with MoO_3 at 42.3%. This recovery suggests that any temporary reduction in activity was overcome as the reaction progressed, possibly due to the regeneration of active sites or the continued separation of charge carriers facilitated by the heterojunction. By 60 min, the photodegradation efficiency was 50.52% for MoO_3. The trend of the composite outperforming the individual catalysts persisted, with the efficiency gap widening. This sustained superiority of the MoO_3 composite can be linked to the continuous generation of ROS and the effective degradation of intermediate dye products that may have formed during the earlier stages (Hussain *et al.,* 2024). At 70 min, the efficiency was 60.8% for MoO_3. In the final stage of photodegradation (80-100 min), the efficiencies of the photocatalysts continued to increase, with 62.16 % for MoO_3. At 90 min, the efficiencies were 71.03% for MoO_3. The ability of the composite to outperform individual components by such a large margin highlights the potential for designing tailored photocatalysts with optimized properties for specific applications. Finally, at 100 min, the photodegradation efficiencies reached 75.25% for MoO_3. A similar report was performed by Gautam *et al.* (2023) on the fabrication of *Curcuma longa* mediated novel Ni@ZnO/MoO_3 composite anchored with g-C_3N_4 for sunlight-driven photocatalytic activity.

The effect of dosage on the photodegradation of dyeing wastewater using MoO_3 is presented in Fig. 6. MoO_3 is another semiconductor photocatalyst known for its high oxidation states and ability to generate reactive oxygen species. At a catalyst loading of 0.25 g, MoO_3 achieves an efficiency of 40.52%, which is lower than that of ZnO at the same loading. This difference can be attributed to the lower photocatalytic activity of MoO_3 under similar conditions, possibly due to its narrower bandgap or less effective charge separation compared to ZnO. For instance, it has been reported that various morphologies of MoO_3, such as nanobelts and nanorods, exhibit low photocatalytic activity, primarily because of the wide bandgap that restricts the absorption of visible light (Sun *et al.,* 2023). As the catalyst loading increases, the efficiency of MoO_3 improves, reaching 50.06% at 0.3 g and 61.1% at 0.35 g. These values are still lower than those observed for other literature such as ZnO, indicating that MoO_3 may require a higher catalyst loading or longer irradiation time to achieve degradation levels like ZnO. At 0.4 g, the efficiency of MoO_3 rises to 79.4%, showing a significant improvement. At 0.45 g, MoO_3 achieves a photodegradation efficiency of 90.85%. Finally, at 0.5 g, the efficiency of MoO_3 reaches 96.9%, which is nearly complete degradation. This slight difference suggests that while MoO_3 is a competent photocatalyst, ZnO is more efficient under the given experimental conditions (Sun *et al.,* 2023).

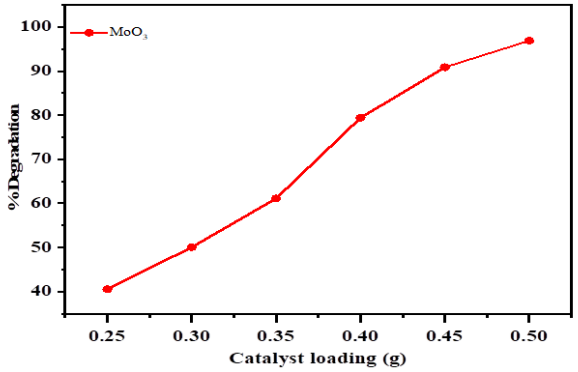

Figure 6: Effect of catalyst loading using MoO_3 under UV-visible light

The photodegradation of dyeing wastewater was assessed at six different pH levels (2, 4, 6, 8, 10, and 12) using MoO_3 photocatalysts (see Fig 7). The results demonstrate a consistent increase in degradation efficiency as the pH increases. The efficiency of photodegradation generally increases with the pH level for the MoO_3 photocatalysts. At pH 2, the degradation efficiencies are relatively low, with MoO_3 at 15.48%. As the pH increases to 12, there is a significant rise in degradation efficiency with MoO_3 at 60.65% reaching the highest efficiency of 77.95%.

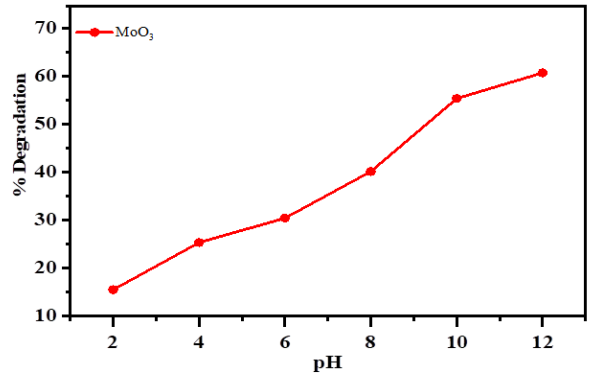

Figure 7: Effect of pH using MoO_3 under UV-visible light

MoO_3 is another semiconductor that has been explored for photocatalytic applications. The performance of MoO_3 in this study shows a similar trend to that of ZnO reported by Pascariu et al., (2020), with increasing degradation efficiency as the pH rises. However, at each pH level, MoO_3 consistently exhibits lower photodegradation efficiency. This lower efficiency can be attributed to the narrower bandgap of MoO_3 which limits its ability to generate enough electron-hole pairs under UV light (Pascariu *et al.* 2020). Moreover, MoO_3 has a lower conduction band edge, which might result in less effective reduction processes. Despite these limitations, the increase in efficiency with pH indicates that MoO_3 also benefits from higher pH levels due to enhanced •OH radical formation.

Conclusion

The study successfully synthesized and characterized MoO_3 nanoparticles for the photocatalytic degradation of dyeing wastewater, demonstrating their efficiency as a sustainable treatment solution. The prepared nanoparticles exhibited excellent structural and optical properties, as evidenced by XRD, SEM, EDX and TEM analyses, confirming their suitability for photocatalysis. The photocatalytic experiments revealed that MoO_3 nanoparticles effectively degraded organic dyes under simulated UV-visible, achieving significant removal efficiencies within short reaction times. Factors such as the effect of catalyst loading, pH, and time were optimized to maximize performance, with higher dosages and UV-visible conditions favouring enhanced degradation. These findings establish MoO_3 nanoparticles as a promising material for addressing the environmental challenges posed by dyeing industry effluents.

REFERENCES

Alsukaibi, A. K. D. (2022). Various approaches for the detoxification of toxic dyes in wastewater. *Processes, 10*(10), 1968. https://doi.org/10.3390/pr10101968

da Silva-Júnior, M. G., Arzuza, L. C. C., Sales, H. B., Farias, R. M. D. C., Neves, G. A., Lira, H. L., & Menezes, R. R. (2023). A Brief Review of MoO_3 and MoO_3-Based Materials and Recent Technological Applications in Gas Sensors, Lithium-Ion Batteries, Adsorption, and Photocatalysis. *Materials (Basel, Switzerland)*, *16*(24), 7657. https://doi.org/10.3390/ma16247657

Dargahi, M., Masteri-Farahani, M., Shahsavarifar, S., & Feizi, M. (2020). Microemulsion-mediated preparation of $Ce_2(MoO_4)_3$ nanoparticles for photocatalytic degradation of crystal violet in aqueous solution. *Environmental science and pollution research international*, *27*(11), 12047–12054. https://doi.org/10.1007/s11356-020-07816-2

Delletesse, M. I., Pompei, M. C., Eyler, G. N., & Nesprías, R. K. (2023). Ecology treatment of a real industrial effluent with chitosan: characterization and design of coagulation-flocculation process. Afinidad. Journal of Chemical Engineering Theoretical and Applied Chemistry, 80(600). https://doi.org/10.55815/422668

Dostanić, J., Lončarević, D., Hadnađev-Kostić, M., & Vulić, T. (2024). Recent Advances in the Strategies for Developing and Modifying Photocatalytic Materials for Wastewater Treatment. *Processes*, *12*(9), 1914. https://doi.org/10.3390/pr12091914

Gautam, N., Singh, K. B., Upadhyay, D. D., Srivastava, S., & Pandey, G. (2023). Fabrication of Curcuma longa mediated novel Ni@ ZnO/MoO_3 composite anchored with g-C3N4 for sunlight driven photocatalytic activity. *Optical Materials*, *142*, 114041.

Gavrilova, N., Myachina, M., Harlamova, D., & Nazarov, V. (2020). Synthesis of Molybdenum Blue Dispersions Using Ascorbic Acid as Reducing Agent. *Colloids and Interfaces*, *4*(2), 24. https://doi.org/10.3390/colloids4020024

Harini, R., Hke, L., & Manjunatha, C. (2022). Impact of green synthesized copper doped nanostructured molybdenum oxide flakes on micro structural, electrical, and electrochemical properties. ECS Transactions, 107(1), 15141-15154. https://doi.org/10.1149/10701.15141ecst

Hendrix, Y., Rauwel, E., Nagpal, K., Haddad, R., Estephan, E., Boissière, C., & Rauwel, P. (2023). Revealing the Dependency of Dye Adsorption and Photocatalytic Activity of ZnO Nanoparticles on Their Morphology and Defect States. *Nanomaterials (Basel, Switzerland)*, *13*(13), 1998. https://doi.org/10.3390/nano13131998

Hussain, M.K., Khalid, N.R., Tanveer, M., Abbas, A., Ali, F., Hassan, W., Rianna, M., Rahman, S., Hamza, M. and Aslam, M., (2024). Facile fabrication of Z-scheme ZnO/MoO3 heterojunction as an excellent visible-light responsive photocatalyst for the degradation of rhodamine B and alizarin yellow dyes. *Optical Materials*, *148*, p.114794.

Inobeme, A., Mathew, J. T., Jatto, E., Inobeme, J., Adetunji, C. O., Muniratu, M., Onyeachu, B. I., Adekoya, M. A., Ajai, A. I., Mann, A., Olori, E., Akhor, S. O., Eziukwu, C. A., Kelani, T., & Omali, P. I. (2023). Recent advances in instrumental techniques for heavy metal quantification. *Environmental monitoring and*

assessment, *195*(4), 452. https://doi.org/10.1007/s10661-023-11058-3.

Jamil, S., Zahra, G., & Janjua, M. R. S. A. (2022). Morphologically controlled synthesis, characterization, and applications of molybdenum oxide (moo3) nanoparticles. Journal of Physical Organic Chemistry, 36(4). https://doi.org/10.1002/poc.4477

Kedves, E. -Z., Bárdos, E., Ravasz, A., Tóth, Z. -R., Mihálydeákpál, S., Kovács, Z., Pap, Z., & Baia, L. (2023). Photoinhibitive Properties of α-MoO_3 on Its Composites with TiO_2, ZnO, BiOI, AgBr, and Cu_2O. *Materials*, *16*(10), 3621. https://doi.org/10.3390/ma16103621

Kim, K., Yoon, S., Kwon, H. A., & Choi, Y. (2020). Effects of treatment agents during acid washing and pH neutralization on the fertility of heavy metal-impacted dredged marine sediment as plant-growing soil. *Environmental Pollution*, *267*, 115466.

Larciprete, M. (2024). Large-area polycrystalline α-MoO_3 thin films for ir photonics. Journal of Physics D Applied Physics, 57(13), 135107. https://doi.org/10.1088/1361-6463/ad18f6

Mathew, J. T., Inobeme, A., Musah, M., Azeh, Y., Abdullahi, A., Shaba E. Y., Salihu, A. M., Muhammad, E. B., Josiah, J. G., Jibrin, N. A., Ismail, H., Muhammad, A. I., Maurice, J., Mamman, A. & Ndamitso, M. M. (2024)a. A Critical Review of Green Approach on Wastewater Treatment Strategies. . *Journal of Applied Science and Environmental Management,* 28(2), 363-391. doi: https://dx.doi.org/10.4314/jasem.v28i2.9

Mathew, J. T., Musah, M., Azeh, Y. & Muhammed, M. (2024)b. Development of Fe3O4 Nanoparticles for the Removal of Some Toxic Metals from Pharmaceutical Wastewater. Caliphate Journal of Science & Technology (CaJoST), 6(1), 26-34. Doi: https://dx.doi.org/10.4314/cajost.v6i1.4

Mathew, J. T., Musah, M., Azeh, Y. & Muhammed, M. (2023)a. Kinetic Study of Heavy Metals Removal from Pharmaceutical Wastewater Using Geopolymer/Fe_3O_4 Nanocomposite. Bima Journal of Science and Technology, 7(4), 152- 163. Doi: 10.56892/bima.v7i4.539.

Mathew, J. T., Musah, M., Azeh, Y. & Muhammed, M. (2023)b. Adsorptive Removal of Selected Toxic Metals from Pharmaceutical Wastewater using Fe_3O_4/ZnO Nanocomposite, *Dutse Journal of Pure and Applied Sciences*, 9(4a), 236- 248. https://dx.doi.org/10.4314/dujopas.v9i4a.22.

Mohamed, W., El-Gawad, H.A., Handal, H., Galal, H., Mousa, H., El-Sayed, B., Mekkey, S., Ibrahem, I. and Labib, A., 2022. Remarkable recycling process of ZnO quantum dots for photodegradation of reactive yellow dye and solar photocatalytic treatment process of industrial wastewater. *Nanomaterials*, *12*(15), p.2642.

Mousavi, S. M., Meraji, S. H., Sanati, A. M., & Ramavandi, B. (2023). Phenol red dye removal from wastewater using TiO_2-FSM-16 and Ni-FSM-16 photocatalysts. *Heliyon*, *9*(3), e14488. https://doi.org/10.1016/j.heliyon.2023.e14488

Mukarugwiro, J. A., Newete, S. W., Nsanganwimana, F., & Byrne, M. J. (2023). Water turbidity affects the establishment of Neochetina eichhorniae (Warner)(Coleoptera: Curculionidae): Implications for biological control of water hyacinth. *Environmental Research*, *237*, 116946.

Norouzi, N., Omo-Lamai, D., Alimohammadi, F., Averianov, T., Kuang, J., Yan, S., Wang, L., Stavitski, E., Leshchev, D., Takeuchi, K. J., Takeuchi, E. S., Marschilok, A. C., Bock, D. C., & Pomerantseva, E. (2022). The Dopamine Assisted Synthesis of MoO_3/Carbon Electrodes With Enhanced Capacitance in Aqueous Electrolyte. *Frontiers in chemistry*, *10*, 873462. https://doi.org/10.3389/fchem.2022.873462

Papadimitropoulos, G., Balliou, A., Kouvatsos, D., & Davazoglou, D. (2022). Gas sensing investigation of porous hot-wire molybdenum disulphide thin films. Advanced Materials Letters, 13(1), 2201-1689. https://doi.org/10.5185/amlett.2022.011689

Pascariu, P., Homocianu, M., Olaru, N., Airinei, A., & Ionescu, O. (2020). New electrospun ZnO: MoO_3 nanostructures: Preparation, characterization and photocatalytic performance. *Nanomaterials*, *10*(8), 1476.

Periyasamy, A. P. (2024). Recent advances in the remediation of textile-dye-containing wastewater: Prioritizing human health and sustainable wastewater treatment. Sustainability, 16(2), 495. https://doi.org/10.3390/su16020495

Qing, Y., Yang, K., Chen, Y., Zhu, J., Li, Y., Chen, C., Li, Q., Sun, B., & He, J. (2023). Thermal Stability, Optical and Electrical Properties of Substoichiometric Molybdenum Oxide. *Materials*, *16*(7), 2841. https://doi.org/10.3390/ma16072841

Rudaru, D., Lucaciu, I., & Fulgheci, A. (2022). Correlation between BOD and COD – biodegradability indicator of wastewater. Romanian Journal of Ecology & Environmental Chemistry, 4(2), 80-86. https://doi.org/10.21698/rjeec.2022.207

Saha, T., Uddin, Z., Islam, M., Shamsuzzaman, M., Tahsin, A., & Islam, M. (2022). Assessing the effectiveness and environmental sustainability of reactive dyes for their structural diversity. Textile & Leather Review, 5, 103-119. https://doi.org/10.31881/tlr.2022.02

Sinar-Mashuri, S. I., Ibrahim, M. L., Kasim, M. F., Mastuli, M. S., Rashid, U., Abdullah, A. H., Islam, A., Asikin Mijan, N., Tan, Y. H., Mansir, N., Mohd Kaus, N. H., & Yun Hin, T. -Y. (2020). Photocatalysis for Organic Wastewater Treatment: From the Basis to Current Challenges for Society. *Catalysts*, *10*(11), 1260. https://doi.org/10.3390/catal10111260

Solomon, C., Dugan, H., Hintz, W., & Jones, S. (2023). Upper limits for road salt pollution in lakes. Limnology and Oceanography Letters, 8(6), 859-866. https://doi.org/10.1002/lol2.10339

Sun, G., Yang, D., Zhang, Z., Wang, Y., Lu, W., & Feng, M. (2023). Oxygen vacancy-rich MoO3 nanorods as photocatalysts for photo-assisted Li-O_2 batteries. *Journal of Advanced Ceramics*, *12*(4), 24-45.

Wang, B. B. (2021). Research on drinking water purification technologies for household use by reducing total dissolved solids (TDS). *Plos one*, *16*(9), e0257865.

Wang, F., Tan, J., He, Y., Quan, Y., & Cui, X. (2023). Preparation of fe-lignin/geopolymer porous microspheres for catalytic degradation of dye wastewater. Industrial &Amp; Engineering Chemistry Research, 62(19), 7763-7768. https://doi.org/10.1021/acs.iecr.3c00404

Xiao, Q., Guo, J., Lu, Y., Gao, J., Jia, C., Huang, M., Chu, W., Yao, W., Ning, P., Xu, Q., & Xu, N. (2024). Molybdenum Nanoparticles Alleviate MC903-Induced Atopic Dermatitis-Like Symptoms in Mice by Modulating the ROS-Mediated NF-κB and Nrf2 /HO-1 Signaling Pathways. *International journal of nanomedicine*, *19*, 8779–8796. https://doi.org/10.2147/IJN.S472999